

Long non-coding RNA *DEPDC1-AS1* promotes proliferation and migration of human gastric cancer cells HGC-27 via the human antigen R-F IIR pathway

Wei Xu^{1,*}, Juan Wang^{2,*}, Jinfu Xu³, Shenyi Li²,
Ranran Zhang², Cong Shen⁴, Min Xie⁵,
Bo Zheng^{4,†}  and Menghui Gu^{1,†}

Abstract

Objective: Long non-coding (lnc) RNAs are critical regulators in carcinogenesis. The novel lncRNA *DEPDC1* antisense RNA 1 (*DEPDC1-AS1*) was recently associated with poor prognosis in triple-negative breast cancer and lung adenocarcinoma. However, its role in regulating the malignant progression of gastric cancer (GC) and its molecular mechanism are unclear. We herein explored the functions of *DEPDC1-AS1* in GC progression.

Methods: *DEPDC1-AS1* expression and prognosis in GC tissues were examined by bioinformatics analysis and quantitative reverse transcription polymerase chain reaction. The *DEPDC1-AS1* function in GC cells was explored by the cell counting kit-8 assay, colony formation assay,

¹Department of Gastrointestinal Surgery, Suzhou Municipal Hospital, The Affiliated Suzhou Hospital of Nanjing Medical University, Gusu School, Nanjing Medical University, Suzhou 215002, China

²Department of Obstetrics and Gynecology, Human Reproductive and Genetic Center, Affiliated Hospital of Jiangnan University, Wuxi 214062, China

³State Key Laboratory of Reproductive Medicine, Department of Histology and Embryology, Nanjing Medical University, Nanjing 211166, China

⁴State Key Laboratory of Reproductive Medicine, Center for Reproduction and Genetics, Suzhou Municipal Hospital, The Affiliated Suzhou Hospital of Nanjing Medical University, Gusu School, Nanjing Medical University, Suzhou 215002, China

⁵The Central Laboratory of Birth Defects Prevention and Control, Ningbo Women and Children's Hospital, Ningbo 315012, China

*These authors contributed equally to this work.

†These authors contributed equally to this work.

Corresponding author:

Menghui Gu, Department of Gastrointestinal Surgery, Suzhou Municipal Hospital, The Affiliated Suzhou Hospital of Nanjing Medical University, Gusu School, Nanjing Medical University, No. 26 Daoqian Street, Suzhou 215002, China.

Emails: cello22444@qq.com



Transwell assay, terminal deoxynucleotidyl transferase-mediated dUTP nick-end labeling, 5-ethyl-2'-deoxyuridine-incorporation, and the xenograft tumor model. The *DEPDC1-AS1* and human antigen (Hu)R interaction was determined by RNA pull-down and RNA immunoprecipitation.

Results: *DEPDC1-AS1* was overexpressed in GC tissues and cell lines, and associated with a worse prognosis in GC patients. *In vitro* and *in vivo* assays showed that *DEPDC1-AS1* promoted HGC-27 cell proliferation and migration. Mechanistically, *DEPDC1-AS1* served as a scaffold by combining with HuR to target the specific mRNA F1IR.

Conclusion: *DEPDC1-AS1* plays a crucial role in GC development and progression and is a potential biomarker for the early detection or prognosis of GC.

Keywords

Gastric cancer, long non-coding RNA, *DEPDC1* antisense RNA 1, human antigen R, F1IR, scaffold

Date received: 8 October 2021; accepted: 23 March 2022

Introduction

Gastric cancer (GC) was the fifth most commonly diagnosed cancer type and the fourth most common cause of cancer-related deaths worldwide in 2020.¹ In recent years, GC incidence rates have increased in Eastern Asia, including China, Japan, South Korea, and North Korea.² Indeed, GC has become the third leading cause of malignant tumor deaths in China, with 478,508 estimated new cases diagnosed in 2020, according to data from the World Health Organization.¹ The 5-year survival rate of GC is very low in China because most patients are diagnosed at an advanced stage.³ Moreover, despite recent advances in screening, diagnosis, and treatment, the prognosis of patients with GC is still poor.⁴ This is mainly attributed to the low accuracy of serum tumor biomarkers for GC, such as pepsinogen I (PGI), PGII, and carcinoembryonic antigen.⁵ Therefore, more effective biomarkers for early GC detection and the prediction of prognosis are warranted.

Recent technological advances in molecular biology, especially in transcriptome

sequencing and bioinformatics, have revealed a complex and diverse range of RNA molecules. Thousands of non-coding RNAs (ncRNAs) have been identified, including small ncRNAs such as microRNAs and long ncRNAs (lncRNAs).⁶ LncRNAs are transcripts longer than 200 nucleotides, which are transcribed by RNA polymerase II but not translated into proteins.⁷ They act as key regulators in many biological processes such as the cell cycle, cell proliferation, metabolism, apoptosis, and differentiation.⁸

Human antigen R (HuR, also known as ELAVL1) belongs to the human/embryonic lethal abnormal vision (Hu/ELAVL1) RNA binding protein family.^{9,10} It interacts with and stabilizes mRNAs through binding to U- and AU-rich elements in their 3'-untranslated regions (UTRs).¹¹ HuR is highly expressed in numerous malignant tumors,¹² where it functions as an mRNA stability factor in response to various cancer-associated stressors, and binds to specific target mRNAs and translocates to the cytoplasm.¹³ Recently, HuR was shown to interact with different lncRNAs,¹⁴ as

seen in the lncRNA–RMST interaction in which HuR enhanced DNA methyltransferase 3 mRNA expression.¹⁵ We previously demonstrated that lncRNA LINC00707 interacted with HuR to increase the stability of F11R mRNA, which is associated with GC cell proliferation and metastasis,¹⁶ indicating that HuR–F11R is a critical pathway involved in GC malignant progression.

In the current study, we identified and characterized a novel lncRNA, *DEPDC1 antisense RNA 1 (DEPDC1-ASI)*, which is considered to be a prognosis predictor for triple-negative breast cancer¹⁷ and lung adenocarcinoma.¹⁸ A comprehensive analysis of The Cancer Genome Atlas (TCGA) database and paired GC and healthy tissues demonstrated that *DEPDC1-ASI* was markedly elevated in human GC tissues, while *DEPDC1-ASI* overexpression was associated with poor prognosis in patients with GC. Functional assays revealed that *DEPDC1-ASI* silencing inhibited GC cell proliferation and migration. Mechanistically, HuR was confirmed as a target of *DEPDC1-ASI* that enhanced F11R mRNA stability. This study offers a better understanding of *DEPDC1-ASI*-associated regulatory modes in the development and progression of GC.

Materials and methods

Human tissues

Paired GC tissues and healthy adjacent tissues were obtained from 24 patients who underwent GC surgery at The Affiliated Suzhou Hospital of Nanjing Medical University between March 2019 and May 2021. Tissue specimens were stored in liquid nitrogen. This study was approved by the Ethics Committee of The Affiliated Suzhou Hospital of Nanjing Medical University (GSKY0233). Patients provided their written informed consent to participate in the study.

Bioinformatics analysis

GC gene expression data were downloaded from the TCGA dataset and analyzed as previously described.¹⁶ The interaction between *DEPDC1-ASI* and HuR was predicted by RNA–Protein Interaction Prediction (RPISeq) (<http://pridb.gdcb.iastate.edu/RPISeq/>).

Cell culture and transfection

Human GC cell lines (HGC-27, Hs746T, NCI-N87, and AGS) and the normal human gastric mucosal epithelial cell line GES-1 were obtained from the Chinese Academy of Cell Collection (Shanghai, China). Cells were cultured in RPMI-1640 medium (Invitrogen, CA, USA) supplemented with 10% fetal bovine serum at 37°C with 5% (v/v) CO₂ in a water-saturated atmosphere.

DEPDC1-ASI and *HuR* small interfering (si)RNAs and the negative control siRNA (si-NC) were transfected into HGC-27 cell lines with Lipofectamine 2000 (Invitrogen). siRNA sequences were as follows: *DEPDC1-ASI* 1#, 5'-AGAUAGGAGAGCACAUGGC-3'; *DEPDC1-ASI* 2#, 5'-UUCUCAGGGUGCAUUAUUC-3'; *HuR* 1#, 5'-UGACCAUUGAAACUGGUAA-3'; *HuR* 2#, 5'-CCUCAAGCCGUUCAGCGUG-3'; and NC, 5'-ACGUGACACGUUCGGAGAA-3'. Additionally, short hairpin (sh)-*DEPDC1-ASI*, pcDNA3.1-*DEPDC1-ASI*, and empty vector were synthesized by GenePharma (Suzhou, China) and transfected with Lipofectamine 2000. Cells were harvested and analyzed at 48 hours post-transfection.

RNA extraction and RT-qPCR assays

Total RNA was extracted from HGC-27, Hs746T, NCI-N87, AGS, and GES-1 cells using TRIzol reagent (Invitrogen). First-strand cDNA was synthesized from total RNA using the PrimeScript RT reagent

(Takara, Dalian, China) according to the manufacturer's instructions. SYBR Taq (Takara)-based quantitative reverse transcription polymerase chain reaction (RT-qPCR) analysis was carried out on a 7500 Real-Time PCR instrument (Applied Biosystems, CA, USA) under the following conditions: 95°C for 5 minutes, then 40 cycles of 95°C for 10 seconds and 58°C for 30 seconds, with a final step at 60°C for 5 minutes. Results were normalized to 18s rRNA expression. The following primers were used: *DEPDC1-AS1*, forward 5'-CGC TCCTCATAGCGAGTCTG-3' and reverse 5'-TGCCAGGATTGTAGTACGCA-3'; *F11R*, forward 5'-ATAGCCGAGGCC ACTTTGAC-3' and reverse 5'-TTCTC CTTCACCTTCGGGCAC-3'; *18sRNA*, forward 5'-AAACGGCTACCACATCCA AG-3' and reverse 5'-CCTCCAAT GGATCCTCGTTA-3'.

CCK-8 and colony formation assays

HGC-27 cells were inoculated into 96-well plates (3000 cells/well). Cell viability was assessed every 24 hours using a Cell Counting Kit-8 (Beyotime, Nantong, China). For colony formation assays, 3×10^3 HGC-27 cells were plated per well of six-well plates and grown for 2 weeks, during which the medium of each well was changed every 3 days. Cells were then harvested and fixed with methanol for 10 minutes before incubating with 0.1% crystal violet staining solution (Beyotime). Visible colonies were counted using ImagePro Plus software (Media Cybernetics, San Diego, CA, USA).

Transwell assays

A total of 2.5×10^4 HGC-27 cells per well were seeded in serum-free medium (Invitrogen) into the upper culture chamber of a 24-well plate with an 8- μ m pore size (Millipore, Billerica, MA, USA). Lower

chamber wells contained a medium supplemented with 20% fetal bovine serum. After incubation for 48 hours, cells on the upper membrane were removed, whereas those on the lower membrane surface were harvested and stained with 0.1% crystal violet.

5-ethynyl-2'-deoxyuridine (EdU) and terminal deoxynucleotidyl transferase-mediated dUTP nick end labeling (TUNEL) experiments

EdU experiments were carried out using an EdU labeling/detection kit (Ribobio, Guangzhou, China) following the manufacturer's protocol. In brief, transfected cells were incubated with 50 μ M EdU labeling medium for 2 hours, then fixed with 4% paraformaldehyde, and permeabilized using 0.2% Triton X-100. Subsequently, cells were reacted with an anti-EdU working solution. Finally, EdU-positive cells were observed and counted under a Zeiss LSM800 confocal laser microscope (Zeiss, Oberkochen, Germany).

The TUNEL assay was performed using an apoptosis detection kit (Vazyme, Nanjing, China), as described previously.¹⁹ Fluorescence microscopy was used to observe and count TUNEL-positive cells.

In vivo assays

Female athymic BALB/c nude mice (4 weeks old) were maintained under specific pathogen-free condition and manipulated according to protocols approved by the Animal Care and Use Committee of Nanjing Medical University. For the cell proliferation assay, 100 μ l of suspended HGC-27 cells transfected with sh-DEPDC1-AS1 or sh-NC at a concentration of 1×10^7 cells/mL were injected subcutaneously into the flanks of athymic BALB/c nude mice ($n = 6$). Tumors were measured every 3 days, and tumor volumes were calculated by the formula: $V = 0.5 \times D \times d^2$

(where V = volume; D = longitudinal diameter; and d = latitudinal diameter). After 15 days, mice were euthanized, and the subcutaneous tumors were obtained and imaged. Animal experiments were approved by the Committee on the Ethics of Animal Experiments of Nanjing Medical University (IACUC-2004020).

In vitro transcription, RNA pull-down assay, and western blotting analysis

In vitro transcription assays were performed using the RiboTM RNAmix-T7 Biotin RNA Labeling Kit (Ribobio). In brief, *DEPDC1-AS1* was transcribed using T7 RNA polymerase and labeled with biotin. RNA pull-down experiments were performed using the PierceTM Magnetic RNA-Protein Pull-Down Kit following the manufacturer's instructions (Thermo Scientific, Waltham, MA, USA). Pull-down products were separated by sodium dodecyl sulfate–polyacrylamide gel electrophoresis and analyzed by western blotting using an anti-HuR antibody (Proteintech, Chicago, IL, USA), as described previously.^{20,21} The 3' UTR of the androgen receptor RNA provided by the manufacturer was used as the positive control²² and the anti-sense strand of *DEPDC1-AS1* was used as the negative control.

RNA immunoprecipitation (RIP) assays

RIP experiments were performed using a Magna RIPTM RNA-Binding Protein Immunoprecipitation Kit (Millipore) according to the manufacturer's protocol. In brief, HGC-27 cells at 80% to 90% confluency were harvested and lysed in a RIP lysis buffer. The cell extract was incubated with magnetic beads conjugated with the anti-HuR antibody or control IgG overnight at 4°C. Precipitated RNA was purified and subjected to RT-qPCR analysis to

evaluate the interactions between HuR and *DEPDC1-AS1*.

Immunofluorescence

Paraffin-embedded tissues were dewaxed, hydrated, and then subjected to antigen retrieval in 10 mM citrate for 15 minutes. Sections were blocked with 1% bovine serum albumin for 2 hours and then incubated with the anti-Ki67 antibody (Abcam, Cambridge, MA, USA) at a dilution of 1:200 overnight at 4°C and the corresponding Alexa-Fluor secondary antibodies (Thermo Scientific) for 1 hour at 37°C. Nuclei were stained with 4',6-diamidino-2-phenylindole (Beyotime), and images were captured using a Zeiss laser confocal microscope (Carl Zeiss, Oberkochen, Germany).

Statistical analysis

The Student's t-test (two-tailed) and one-way analysis of variance were used to analyze differences between groups. Survival curves were drawn by a Kaplan–Meier survival plot and tested with log-rank tests. Gene set enrichment analysis (GSEA) analysis of pathways associated with *DEPDC1-AS1* was based on TCGA dataset. All statistical analyses were conducted using SPSS 17.0 software (SPSS Inc., Chicago, IL, USA). P values less than 0.05 were recognized as statistically significant.

Results

Overexpression of DEPDC1-AS1 is correlated with GC malignant progression and poor prognosis

DEPDC1-AS1 levels were evaluated in 375 human GC and 32 healthy tissues from the TCGA database, and shown to be significantly overexpressed in GC tissues ($P < 0.01$; Figure 1a). GSEA revealed that *DEPDC1-AS1* expression was significantly

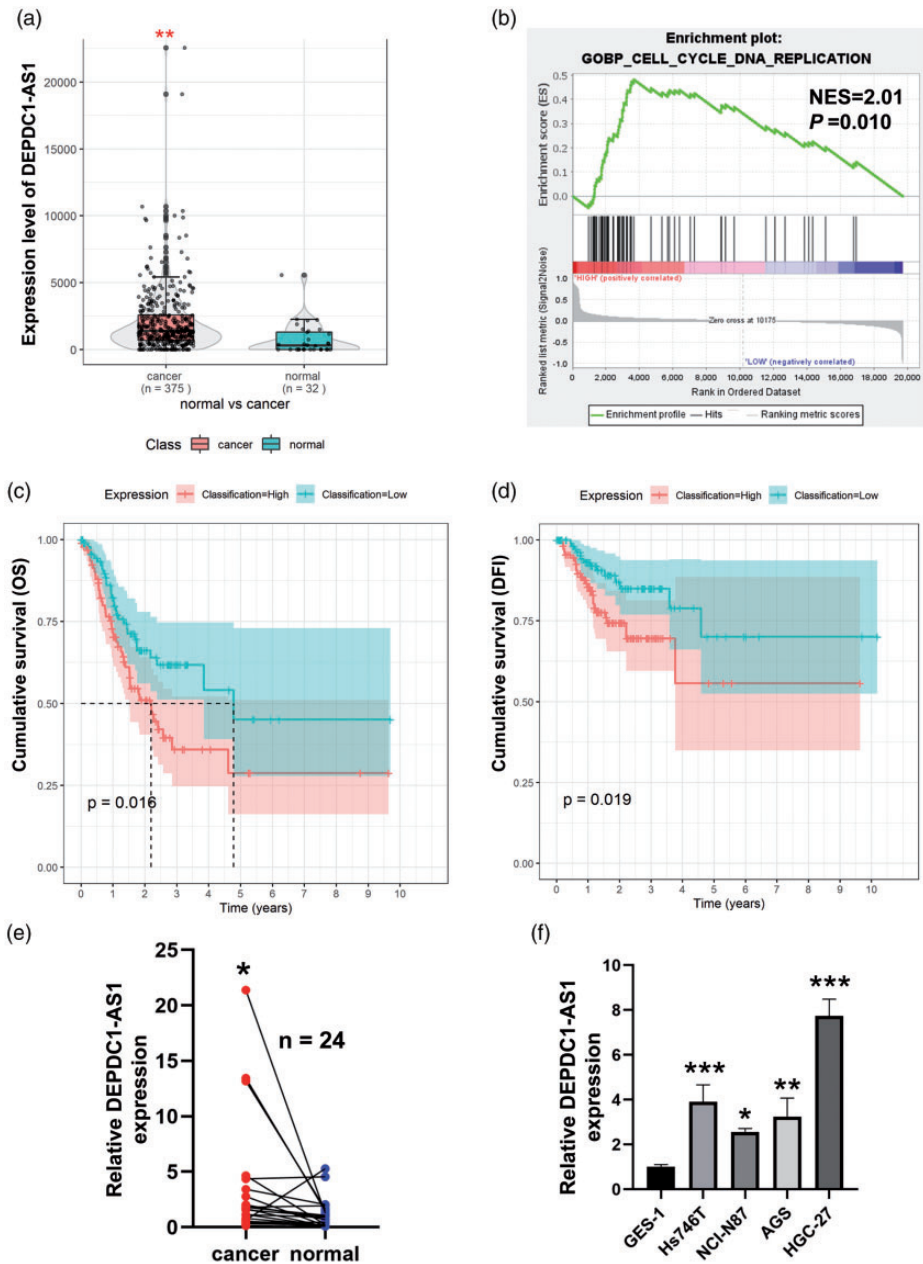


Figure 1. *DEPDC1-AS1* expression in GC tissues and cell lines, and its clinical importance. (a) *DEPDC1-AS1* expression in TCGA database. (b) GSEA analysis of *DEPDC1-AS1* in GC tissues. (c,d) Kaplan–Meier analysis of overall survival and disease-free interval curves in patients with GC. (e) *DEPDC1-AS1* expression in 24 paired GC tissues and healthy adjacent tissues. (f) *DEPDC1-AS1* expression in GC cell lines (HGC-27, Hs746T, NCI-N87, and AGS) and the normal human gastric mucosal epithelial cell line GES-1. n = 3 for each group. * $P < 0.05$, ** $P < 0.01$, *** $P < 0.01$.

DEPDC1 antisense RNA 1, DEPDC1-AS1; GC, gastric cancer; TCGA, the Cancer Genome Atlas; GSEA, gene set enrichment analysis.

positively correlated with the cell cycle and DNA replication in GC tissues ($P=0.01$; Figure 1b). Furthermore, overall survival and disease-free interval curves showed that *DEPDC1-ASI* overexpression was associated with significantly worse prognosis in patients with GC ($P<0.05$; Figure 1c and d). *DEPDC1-ASI* expression was also significantly up-regulated in GC tissues compared with healthy adjacent tissues ($P<0.05$; Figure 1e), and significantly higher in GC cell lines than in the GES-1 cell line ($P<0.05$; Figure 1f). Because *DEPDC1-ASI* expression was highest in HGC-27 cells, we used this cell line for subsequent study.

***DEPDC1-ASI* knockdown suppresses HGC-27 cell proliferation and migration, and promotes apoptosis in vitro**

To investigate the functions of *DEPDC1-ASI* in GC malignant progression, two independent siRNAs (1# and 2#) were transfected into HGC-27 cells, which significantly reduced *DEPDC1-ASI* expression levels ($P<0.01$; Figure 2a). CCK8 and colony formation assays showed significantly impaired cell viability after *DEPDC1-ASI* downregulation ($P<0.001$; Figure 2b–d). Transwell assays revealed that *DEPDC1-ASI* knockdown significantly impaired cell migration when compared with the si-NC group ($P<0.01$; Figure 2e and f).

To further explore the reason for compromised viability in *DEPDC1-ASI* knockdown cells, we performed TUNEL staining and EdU incorporation experiments to test cell proliferation and apoptosis, respectively. TUNEL staining revealed a significant increase in the proportion of TUNEL-positive cells in the interference group compared with the control group ($P<0.05$; Figure 3a and b). In contrast, EdU incorporation showed significantly compromised proliferative activity in *DEPDC1-ASI*-knockdown cells ($P<0.05$; Figure 3c

and d). Taken together, our data suggested that *DEPDC1-ASI* is an oncogene in GC.

***DEPDC1-ASI* knockdown suppresses GC growth in vivo**

To evaluate whether *DEPDC1-ASI* could influence HGC-27 cell tumorigenesis *in vivo*, we injected HGC-27 cells transfected with sh-*DEPDC1-ASI* or its control group (empty vector) into nude mice. In the course of xenograft tumor development, tumor growth was significantly slower in the sh-*DEPDC1-ASI* group compared with the control group ($P<0.05$; Figure 4a). At 15 days postinjection, xenograft tumors grown from sh-*DEPDC1-ASI* cells were significantly smaller and lighter than those from control cells ($P<0.05$; Figure 4b and c). RT-qPCR analysis found that *DEPDC1-ASI* expression levels were significantly decreased in tumor tissues generated from sh-*DEPDC1-ASI* cells ($P<0.01$; Figure 4d). Furthermore, immunofluorescence staining revealed significantly fewer Ki67-positive cells in the tumors of *DEPDC1-ASI* knockdown cells ($P<0.01$; Figure 4e and f).

***DEPDC1-ASI* interacts with the mRNA-stabilizing protein HuR**

To further investigate the molecular mechanisms of *DEPDC1-ASI* in GC progression, we employed RPISeq to predict the interaction between *DEPDC1-ASI* and RNA-binding proteins. *DEPDC1-ASI* was found to potentially bind HuR, as both the RF Classifier and SVM Classifier scores were greater than 0.5 (Figure 5a). Subsequently, RNA pull-down and RIP experiments confirmed the binding between *DEPDC1-ASI* and HuR (Figure 5b and c). In GC, HuR improves the stability of mRNA F11R by interacting with LINC00707.¹⁶ However, whether *DEPDC1-ASI* regulates the HuR–F11R axis is unclear. Therefore, the correlation between *DEPDC1-ASI* and

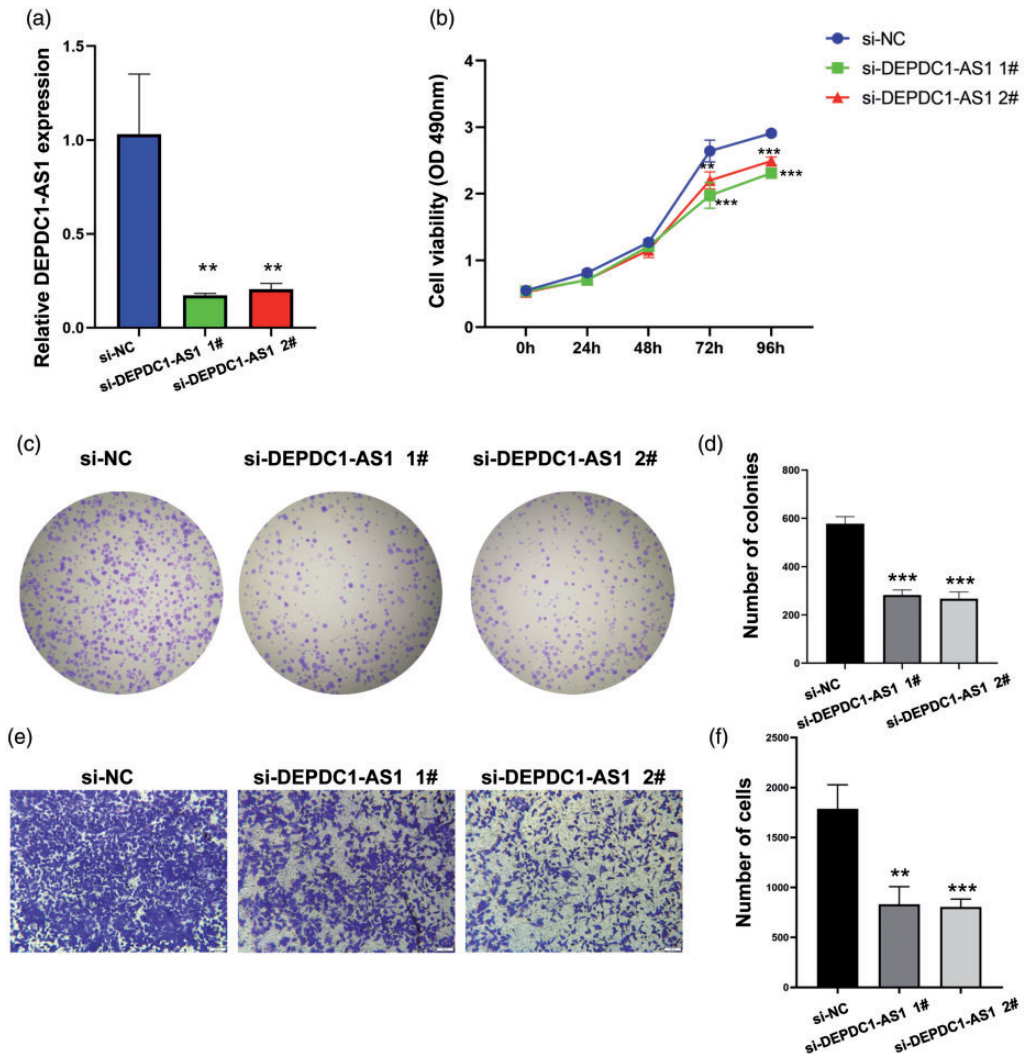


Figure 2. Effects of *DEPDC1-AS1* knockdown on HGC-27 cell viability and migration *in vitro*. (a) *DEPDC1-AS1* expression in HGC-27 cells transfected with si-NC or si-*DEPDC1-AS1* 1# and 2#. $n = 3$ for each group. (b) CCK8 assays in HGC-27 cells transfected with si-NC or si-*DEPDC1-AS1*. $n = 4$ for each group. (c, d) Colony formation assays in HGC-27 cells transfected with si-NC or si-*DEPDC1-AS1*. $n = 3$ for each group. (e, f) Transwell assays in HGC-27 cells transfected with si-NC or si-*DEPDC1-AS1*. $n = 3$ for each group. Scale bar: 100 μm . * $P < 0.01$, ** $P < 0.001$.

DEPDC1 antisense RNA 1, *DEPDC1-AS1*; si, small interfering; CCK, cell counting kit.

the HuR–F11R axis was explored. F11R mRNA expression was significantly down-regulated after *DEPDC1-AS1* or HuR knockdown in HGC-27 cells ($P < 0.001$; Figure 5d). Notably, the interaction between F11R mRNA and HuR was significantly

attenuated when *DEPDC1-AS1* was silenced ($P < 0.05$; Figure 5e). Additionally, correlation analysis showed that F11R expression levels were significantly positively correlated with *DEPDC1-AS1* expression levels in GC tissues ($P < 0.001$; Figure 5f). We therefore

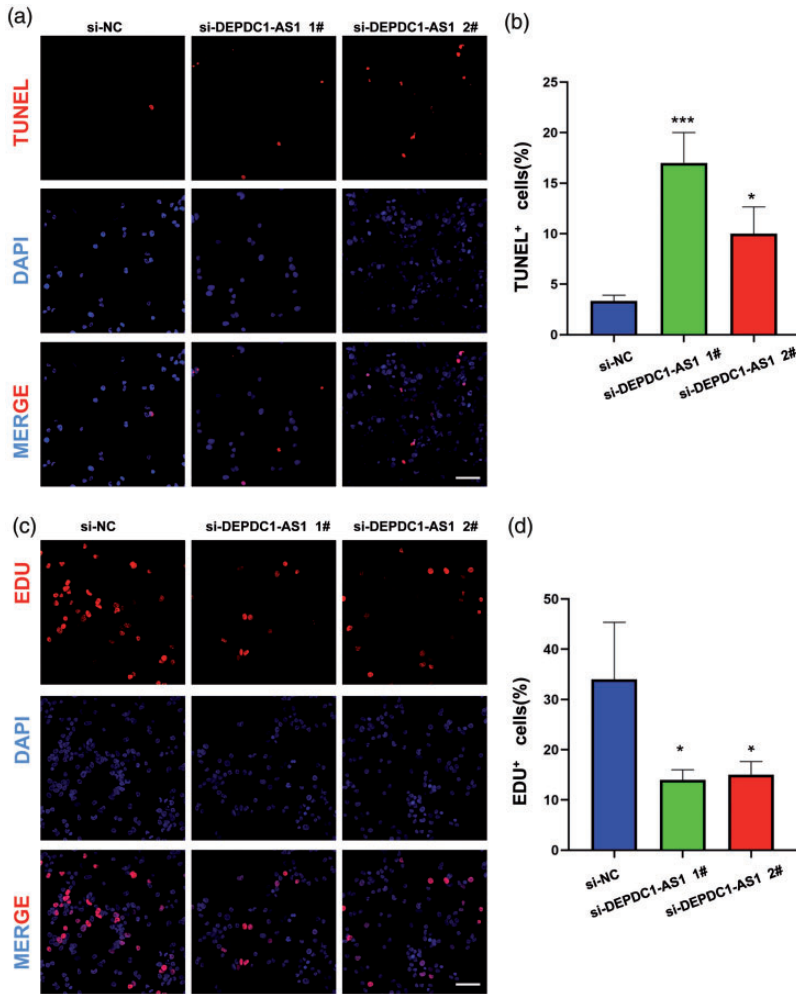


Figure 3. Effects of *DEPDC1-AS1* knockdown on HGC-27 cell proliferation and apoptosis. (a, b) TUNEL staining in HGC-27 cells transfected with si-NC or si-*DEPDC1-AS1*. n = 3 for each group. (c, d) EdU incorporation assay in HGC-27 cells transfected with si-NC or si-*DEPDC1-AS1*. n = 3 for each group. Scale bar: 50 μ m. * $P < 0.05$, *** $P < 0.001$.

DEPDC1 antisense RNA 1, *DEPDC1-AS1*; terminal deoxynucleotidyl transferase-mediated dUTP nick end labelling, TUNEL; si, small interfering; EdU, 5-ethynyl-2'-deoxyuridine.

conclude that *DEPDC1-AS1* is involved in the HuR–F11R co-regulatory effects on GC progression.

F11R is involved in the oncogene function of *DEPDC1-AS1*

We conducted rescue experiments to investigate whether F11R was involved in

DEPDC1-AS1-induced GC cell proliferation and migration. CCK8 and colony formation assay data revealed that co-transfection of *DEPDC1-AS1* siRNA and pcDNA-F11R vector largely rescued *DEPDC1-AS1* knockdown-induced compromised cell viability ($P < 0.01$; Figure 6a–c), and cell migration was also significantly rescued after co-transfection ($P < 0.001$; Figure 6d and e).

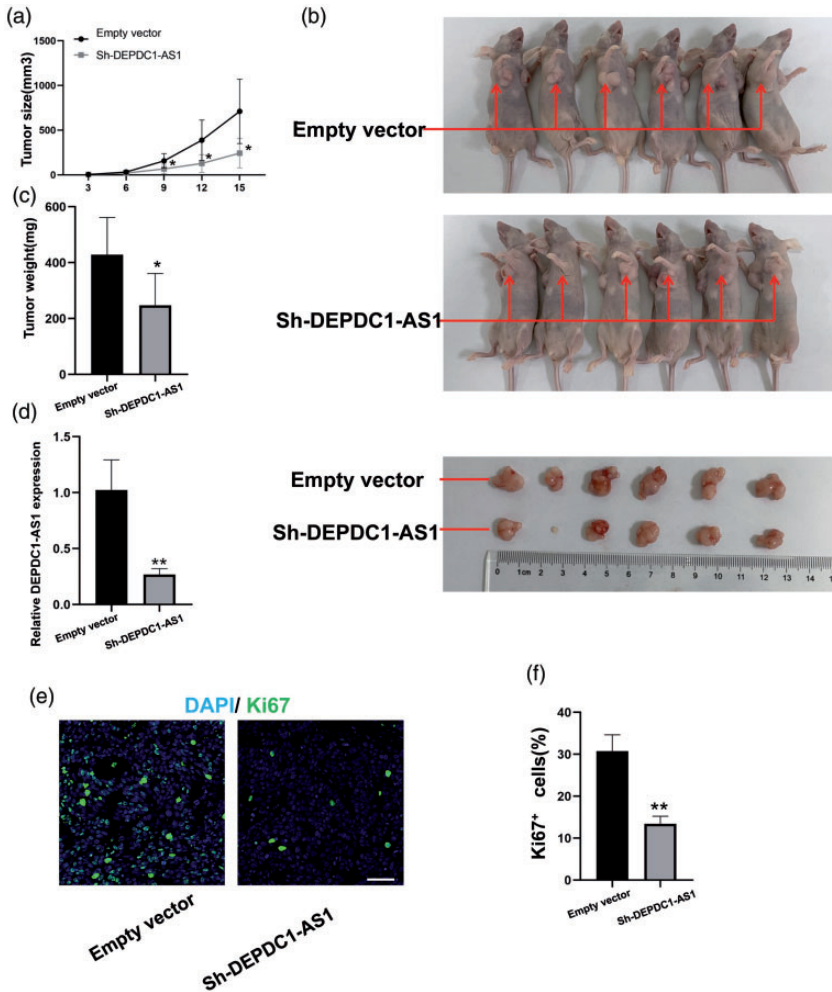


Figure 4. *DEPDC1-AS1* knockdown promoted HGC-27 cell tumorigenesis *in vivo*. Empty vector or sh-*DEPDC1-AS1* were transfected into HGC-27 cells and subcutaneously injected into nude mice. (a) Tumor volumes were measured every 3 days post-injection. (b) Tumors were isolated and photographed. (c) Tumor weights were measured at the end of the experiment. (d) RT-qPCR analysis of *DEPDC1-AS1* expression in tumors. (e, f) Immunostaining of the proliferation index factor Ki67 in tumor sections. Scale bar: 50 μ m. For (a) to (f), $n = 6$ for each group. * $P < 0.05$, ** $P < 0.01$.

DEPDC1 antisense RNA 1, *DEPDC1-AS1*; sh, short hairpin; RT-qPCR, quantitative reverse transcription polymerase chain reaction.

Discussion

GC is one of the most common malignancies worldwide, and several oncogenic pathways that may contribute to GC carcinogenesis have been reported in recent years.^{23,24} Multiple lncRNAs act as

oncogenes or tumor suppressor genes during carcinogenesis and can also serve as prognostic markers of GC.^{25–27} lncRNA-mediated regulation of signaling pathways in cancer has been shown to be involved in various mechanisms, which are mainly attributed to their interaction with

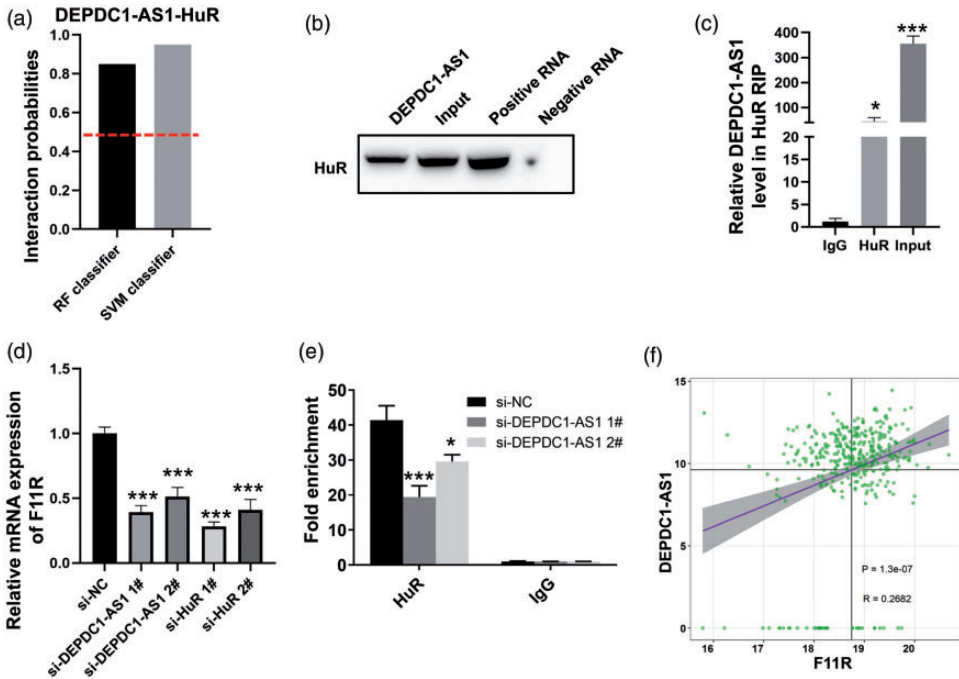


Figure 5. *DEPDC1-AS1* interacts with HuR. (a) RNA–protein interaction prediction between *DEPDC1-AS1* and HuR. An interaction score > 0.5 was considered positive. (b) Western blot analysis of RNA–protein complexes using an anti-HuR antibody. Experiments were repeated twice. (c) RIP experiments of *DEPDC1-AS1* binding to HuR in HGC-27 cell lysates. The relative *DEPDC1-AS1* level in HuR RIP is relative to its control IgG. n = 3 for each group. (d) RT-qPCR analysis of the relative mRNA expression of F11R after *DEPDC1-AS1* or HuR knockdown in HGC-27 cells. n = 3 for each group. (e) The fold enrichment of F11R in HuR RIP after *DEPDC1-AS1* knockdown in HGC-27 cells. The relative *DEPDC1-AS1* level in HuR RIP is relative to its control IgG. n = 3 for each group. (f) Correlation between *DEPDC1-AS1* and F11R expression. * $P < 0.05$, *** $P < 0.001$.

DEPDC1 antisense RNA 1, *DEPDC1-AS1*; HuR, human antigen R; RT-qPCR, quantitative reverse transcription polymerase chain reaction.

DNA, RNA, or protein. These include: (1) targeting specific DNA binding proteins to reduce their access to DNA recognition elements,²⁸ (2) miRNA targeting of lncRNAs to trigger their decay,²⁹ and (3) the selective regulation of mRNA stability of specific genes by interacting with target proteins.²⁸

DEPCE-AS1, a novel lncRNA, was recently associated with the prognosis of triple-negative breast cancer¹⁷ and lung adenocarcinoma.¹⁸ However, changes in the expression of *DEPDC1-AS1* in GC are poorly understood. Here, we found that *DEPDC1-AS1* was overexpressed in GC

tissues and cell lines, while loss-of-function assays verified that excessive *DEPDC1-AS1* promoted HGC-27 cell line proliferation and migration and that this function was attributed to its interaction with HuR. These findings indicate that *DEPDC1-AS1* acts as an oncogene in GC development, and can be used as a potential biomarker of GC prognosis.

F11R, also known as junctional adhesion molecule-A, is a member of the immunoglobulin superfamily originally identified from the surface of human platelets, and is a crucial regulator of tight junction assembly

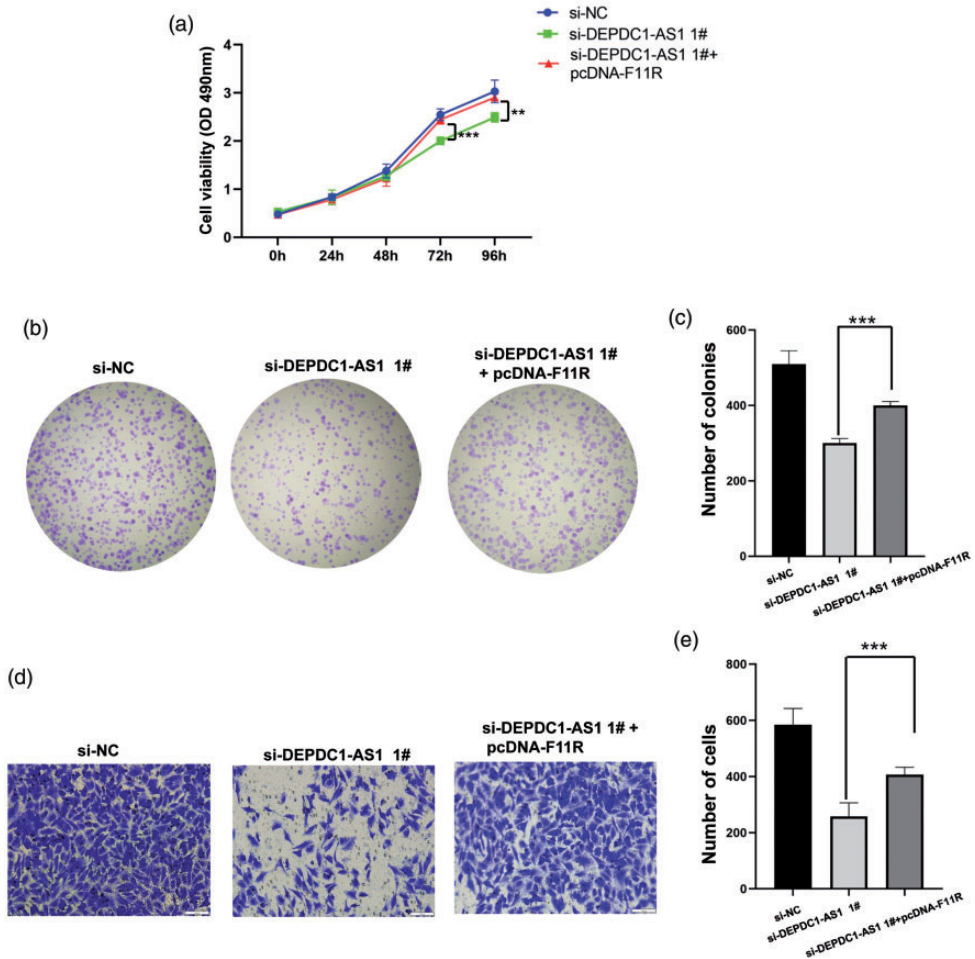


Figure 6. F11R is involved in the oncogene function of *DEPDC1-AS1*. (a) CCK8 assays in NC, si-*DEPDC1-AS1* 1#, and pcDNA-F11R co-transfected HGC-27 cells. n = 4 for each group. (b, c) Colony formation assay in NC, si-*DEPDC1-AS1* 1#, and pcDNA-F11R co-transfected HGC-27 cells. n = 3 for each group. (d, e) Transwell assays in NC, si-*DEPDC1-AS1* 1#, and pcDNA-F11R co-transfected HGC-27 cells. n = 3 for each group. Scale bar: 100 μ m. * $P < 0.01$, *** $P < 0.001$. DEPDC1 antisense RNA 1, DEPDC1-AS1; CCK, cell counting kit; si, small interfering.

in epithelia.^{30,31} Various studies have focused on its role in cancers. These include the hypoxic induction of lncRNA *NEATI*, which leads to the retention of F11R within the nucleus and correlates with poor survival in patients with breast cancer.³¹ Moreover, Zhang et al. revealed that overexpression of F11R mRNA correlated with non-small cell lung cancer progression.^{32,33} We previously

reported an interaction between LINC00707 and HuR in which HuR increased the stability of F11R mRNA, and verified the role of the HuR-F11R pathway in GC malignant progression.¹⁶ This earlier study found that the 3'-UTR of F11R interacted with HuR, while RIP analysis demonstrated the high binding capacity of F11R for HuR protein.¹⁶

The current study confirmed that *DEPDC1-AS1* binds HuR, and showed that it functions as a scaffold to regulate F11R at the transcriptional level. Bioinformatics and mRNA expression analysis revealed a positive correlation between *DEPDC1-AS1* and F11R, which was demonstrated to be a strong binding relationship by RNA pull-down and RIP assays, while *in vitro* loss-of-function assays showed that F11R regulation is potentially involved in the oncogene function of *DEPDC1-AS1*.

In conclusion, our results reveal GC-associated *DEPDC1-AS1* to be an oncogenic lncRNA that promotes the proliferation and invasion of HGC-27 cells by serving as a scaffold, and combines with HuR to target F11R mRNA. Our findings support a role for *DEPDC1-AS1* in GC development and progression and suggest that it could be used as an effective biomarker for the early detection or prognosis of GC.

Declaration of conflicting interest

The authors declare that there is no conflict of interest.

Funding

The authors disclosed receipt of the following financial support for the research, authorship, and publication of this article: This research was supported by the Open Fund of State Key Laboratory of Reproductive Medicine of Nanjing Medical University (SKLRM-K202010), and the Gusu Health Talent Program of Suzhou (GSWS2020068).

ORCID iD

Bo Zheng  <https://orcid.org/0000-0002-1496-0753>

References

1. Sung H, Ferlay J, Siegel RL, et al. Global Cancer Statistics 2020: GLOBOCAN estimates of incidence and mortality worldwide for 36 cancers in 185 countries. *CA Cancer J*

Clin 2021; 71: 209–249. 2021/02/05. DOI: 10.3322/caac.21660.

2. Sugano K. Screening of gastric cancer in Asia. *Best Pract Res Clin Gastroenterol* 2015; 29: 895–905. 2015/12/15. DOI: 10.1016/j.bpg.2015.09.013.
3. Zong L, Abe M, Seto Y, et al. The challenge of screening for early gastric cancer in China. *Lancet (London, England)* 2016; 388: 2606. 2016/11/30. DOI: 10.1016/s0140-6736(16)32226-7.
4. Sawaki K, Kanda M and Kodera Y. Review of recent efforts to discover biomarkers for early detection, monitoring, prognosis, and prediction of treatment responses of patients with gastric cancer. *Expert Rev Gastroenterol Hepatol* 2018; 12: 657–670. 2018/06/15. DOI: 10.1080/17474124.2018.1489233.
5. Miao J, Liu Y, Zhao G, et al. Feasibility of plasma-methylated SFRP2 for early detection of gastric cancer. *Cancer Control* 2020; 27: 1073274820922559. 2020/05/08. DOI: 10.1177/1073274820922559.
6. Lorenzi L, Avila Cobos F, Decock A, et al. Long noncoding RNA expression profiling in cancer: Challenges and opportunities. *Genes, chromosomes & cancer* 2019; 58: 191–199. 2018/11/22. DOI: 10.1002/gcc.22709.
7. Chan JJ and Tay Y. Noncoding RNA:RNA regulatory networks in cancer. *Int J Mol Sci* 2018; 19: 1310 2018/04/28. DOI: 10.3390/ijms19051310.
8. Akhade VS, Pal D and Kanduri C. Long noncoding RNA: genome organization and mechanism of action. *Adv Exp Med Biol* 2017; 1008: 47–74. 2017/08/18. DOI: 10.1007/978-981-10-5203-3_2.
9. Brennan CM and Steitz JA. HuR and mRNA stability. *Cell Mol Life Sci* 2001; 58: 266–277. 2001/04/06. DOI: 10.1007/pl00000854.
10. Huang YH, Peng W, Furuuchi N, et al. Delivery of therapeutics targeting the mRNA-binding protein HuR using 3DNA nanocarriers suppresses ovarian tumor growth. *Cancer Res* 2016; 76: 1549–1559. 2016/02/28. DOI: 10.1158/0008-5472.Can-15-2073.
11. Srikantan S and Gorospe M. HuR function in disease. *Front Biosci (Landmark Ed)*

- 2012; 17: 189–205. 2011/12/29. DOI: 10.2741/3921.
12. López de Silanes I, Lal A and Gorospe M. HuR: post-transcriptional paths to malignancy. *RNA Biol* 2005; 2: 11–13. 2006/11/30. DOI: 10.4161/rna.2.1.1552.
 13. Brody JR and Dixon DA. Complex HuR function in pancreatic cancer cells. *Wiley Interdiscip Rev RNA* 2018; 9: e1469. 2018/02/17. DOI: 10.1002/wrna.1469.
 14. Jonas K, Calin GA and Pichler M. RNA-binding proteins as important regulators of long non-coding RNAs in cancer. *Int J Mol Sci* 2020; 21: 2969. 2020/04/29. DOI: 10.3390/ijms21082969.
 15. Peng WX, Koirala P, Zhang W, et al. lncRNA RMST enhances DNMT3 expression through interaction with HuR. *Mol Ther* 2020; 28: 9–18. 2019/10/23. DOI: 10.1016/j.ymthe.2019.09.024.
 16. Xie M, Ma T, Xue J, et al. The long intergenic non-protein coding RNA 707 promotes proliferation and metastasis of gastric cancer by interacting with mRNA stabilizing protein HuR. *Cancer Lett* 2019; 443: 67–79. 2018/12/07. DOI: S0304-3835(18)30698-0 [pii] 10.1016/j.canlet.2018.11.032.
 17. Yuan C, Yuan H, Chen L, et al. A novel three-long noncoding RNA risk score system for the prognostic prediction of triple-negative breast cancer. *Biomark Med* 2021; 15: 43–55. 2021/01/12. DOI: 10.2217/bmm-2020-0505.
 18. Lu L, Liu LP, Zhao QQ, et al. Identification of a ferroptosis-related lncRNA signature as a novel prognosis model for lung adenocarcinoma. *Front Oncol* 2021; 11: 675545. 2021/07/13. DOI: 10.3389/fonc.2021.675545.
 19. Gao T, Lin M, Shao B, et al. BMI1 promotes steroidogenesis through maintaining redox homeostasis in mouse MLTC-1 and primary Leydig cells. *Cell Cycle* 2020; 19: 1884–1898. 2020/07/01. DOI: 10.1080/15384101.2020.1779471.
 20. Yu J, Wu Y, Li H, et al. BMI1 drives steroidogenesis through epigenetically repressing the p38 MAPK pathway. *Front Cell Dev Biol* 2021; 9: 665089. 2021/05/01. DOI: 10.3389/fcell.2021.665089.
 21. Zhao D, Shen C, Gao T, et al. Myotubularin related protein 7 is essential for the spermatogonial stem cell homeostasis via PI3K/AKT signaling. *Cell Cycle* 2019; 18: 2800–2813. 2019/09/04. DOI: 10.1080/15384101.2019.1661174.
 22. Yeap BB, Voon DC, Vivian JP, et al. Novel binding of HuR and poly(C)-binding protein to a conserved UC-rich motif within the 3'-untranslated region of the androgen receptor messenger RNA. *J Biol Chem* 2002; 277: 27183–27192. 2002/05/16. DOI: 10.1074/jbc.M202883200 S0021-9258(18)60065-1 [pii].
 23. Wei L, Sun J, Zhang N, et al. Noncoding RNAs in gastric cancer: implications for drug resistance. *Mol Cancer* 2020; 19: 62. 2020/03/21. DOI: 10.1186/s12943-020-01185-7.
 24. Ghafouri-Fard S and Taheri M. Long non-coding RNA signature in gastric cancer. *Exp Mol Pathol* 2020; 113: 104365. 2020/01/04. DOI: 10.1016/j.yexmp.2019.104365.
 25. Sun TT, He J, Liang Q, et al. lncRNA GCIncl promotes gastric carcinogenesis and may act as a modular scaffold of WDR5 and KAT2A complexes to specify the histone modification pattern. *Cancer Discov* 2016; 6: 784–801. 2016/05/06. DOI: 10.1158/2159-8290.Cd-15-0921.
 26. Zhang E, He X, Zhang C, et al. A novel long noncoding RNA HOXC-AS3 mediates tumorigenesis of gastric cancer by binding to YBX1. *Genome Biol* 2018; 19: 154. 2018/10/06. DOI: 10.1186/s13059-018-1523-0.
 27. Sun M, Nie F, Wang Y, et al. lncRNA HOXA11-AS promotes proliferation and invasion of gastric cancer by scaffolding the chromatin modification factors PRC2, LSD1, and DNMT1. *Cancer Res* 2016; 76: 6299–6310. 2016/11/03. DOI: 10.1158/0008-5472.Can-16-0356.
 28. Peng WX, Koirala P and Mo YY. lncRNA-mediated regulation of cell signaling in cancer. *Oncogene* 2017; 36: 5661–5667. 2017/06/13. DOI: 10.1038/onc.2017.184.
 29. Li J, Meng H, Bai Y, et al. Regulation of lncRNA and its role in cancer metastasis. *Oncol Res* 2016; 23: 205–217. 2016/04/22. DOI: 10.3727/096504016x14549667334007.
 30. Ben-Zvi M, Amariglio N, Paret G, et al. F11R expression upon hypoxia is regulated by RNA editing. *PLoS One* 2013; 8: e77702.

- 2013/10/23. DOI: 10.1371/journal.pone.0077702.
31. Choudhry H, Albukhari A, Morotti M, et al. Tumor hypoxia induces nuclear paraspeckle formation through HIF-2alpha dependent transcriptional activation of NEAT1 leading to cancer cell survival. *Oncogene* 2015; 34: 4482–4490. 2014/11/25. DOI: 10.1038/onc.2014.378 onc2014378 [pii].
32. Zhang M, Luo W, Huang B, et al. Overexpression of JAM-A in non-small cell lung cancer correlates with tumor progression. *PLoS One* 2013; 8: e79173. 2013/11/23. DOI: 10.1371/journal.pone.0079173.
33. Kakuki T, Kurose M, Takano K, et al. Dysregulation of junctional adhesion molecule-A via p63/GATA-3 in head and neck squamous cell carcinoma. *Oncotarget* 2016; 7: 33887–33900. 2016/04/02. DOI: 10.18632/oncotarget.8432.